OL Organic Letters

pubs.acs.org/OrgLett Letter

# Oxyquinoliziniporphyrins: Introduction of a Heterocyclic Dimension to Carbaporphyrinoid Systems

Emma K. Cramer, Deyaa I. AbuSalim, and Timothy D. Lash*

Cite This: *Org. Lett.* 2022, 24, 5402−5406 Read Online

ACCESS | Metrics & More | Article Recommendations | Supporting Information

**ABSTRACT:** Oxyquinoliziniporphyrins, novel carbaporphyrinoids that incorporate quinolizone units, were synthesized. These structures exhibit moderate diamagnetic ring currents that are greatly enhanced upon protonation. Addition of trifluoroacetic acid initially gave a monocation, but this was readily converted into a dicationic species. The aromatic character of the free base and protonated species was assessed by proton NMR, nucleus-independent chemical shift calculations, and anisotropy of induced ring current plots. Stable Ni(II) and Pd(II) complexes are also reported.

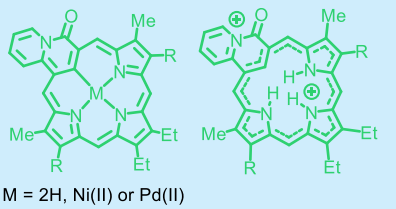




Carbaporphyrinoid systems in which a porphyrin-like framework has one or more of the usual pyrrolic nitrogens replaced with carbon atoms have attracted widespread attention due to their intriguing reactivity and spectroscopic properties, together with their ability to form stable organometallic derivatives.[1] True carbaporphyrins such as **1** and **2** (Figure 1) are trianionic ligands that afford Ag(III), Au(III), Ir(III), and Rh(III) complexes.[2,3] However, related systems such as azuliporphyrins **3**[4] and benziporphyrins **4**[5] commonly act as dianionic ligands giving Ni(II), Pd(II), and Pt(II) complexes. N-Confused porphyrins (NCPs, **5**) are a particularly well studied group of carbaporphyrinoids due to their accessibility and ability to form a wide range of derivatives.[6,7] The interesting chemistry associated with NCPs is due in large measure to the presence of an external nitrogen atom in this system. Other examples of carbaporphyrinoids with external heteroatoms are known, including pyrazoloporphyrins **6**[8] and "N-confused" pyriporphyrins,[9] but investigations in this area have been limited. In this study, the synthesis of carbaporphyrin analogues **7** incorporating a 4-quinolizone unit has been accomplished (Scheme 1).

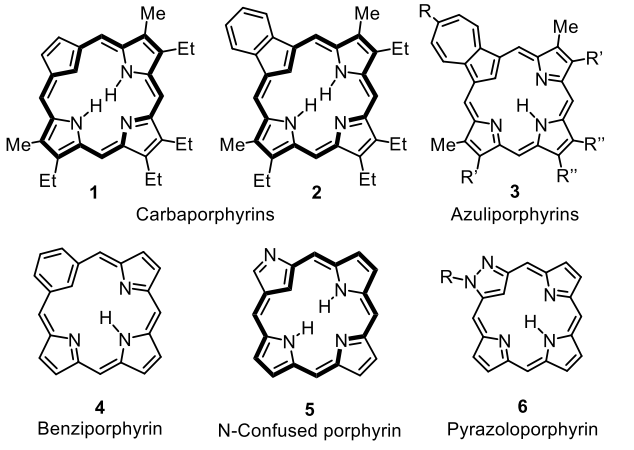


**Figure 1.** Selected carbaporphyrihnoid systems.

**Scheme 1. Synthesis of Oxyquinoliziniporphyrins**

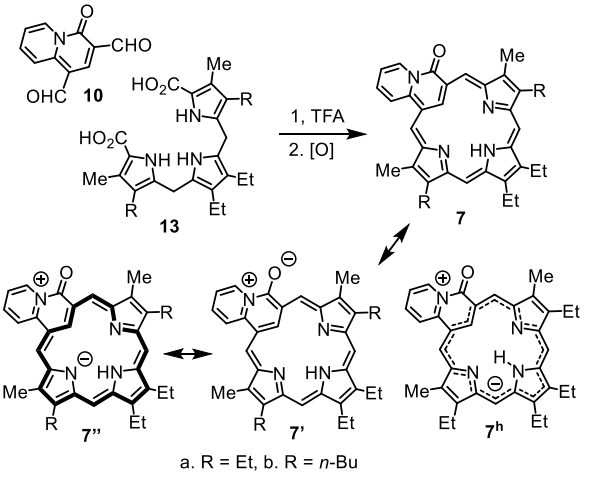


Quinolizinium ions **8** are cationic heterocycles possessing a bridgehead nitrogen, while 4-quinolizone **9** is a related pyridinone-like structure (Figure 2).[10] Although 4-quinolizone is cross-conjugated and formally nonaromatic, dipolar resonance contributor **9′** incorporates an aromatic quinolizinium ion. This interplay between aromaticity and nonaromatic

**Received:** June 21, 2022
**Published:** July 17, 2022





https://doi.org/10.1021/acs.orglett.2c02098
*Org. Lett.* 2022, 24, 5402−5406

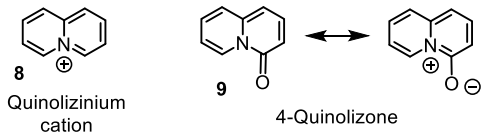


**Figure 2.** Structures of the quinolizinium cation and 4-quinolizone.

character makes this structural unit intriguing and therefore a desirable component for a carbaporphyrin-like system.

Quinolizone dialdehyde **10** was required to synthesize the targeted porphyrinoids, and this was prepared in three steps from pyridylacetate **11** (Scheme 2). Reaction with diethyl

**Scheme 2. Synthesis of a Quinolizone Dialdehyde**

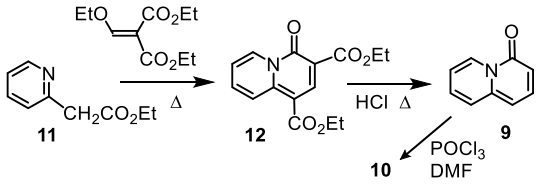


ethoxymethylenemalonate gave diester **12**, and subsequent hydrolysis in refluxing hydrochloric acid afforded quinolizone **9**.[11] Finally, Vilsmeier−Haack formylation furnished dialdehyde **10** in 89% yield. Condensation of **10** with tripyrrane **13a** in TFA−$CH_2Cl_2$, followed by oxidation with 2,3-dichloro-5,6-dicyano-1,4-benzoquinone (DDQ) gave oxyquinoliziniporphyrin **7a** in 54% yield (Scheme 1). However, the macrocyclic product proved to be highly insoluble in organic solvents, and this only allowed limited spectroscopic analysis. In order to overcome this difficulty, *n*-butyl-substituted porphyrinoid **7b** was prepared by reacting dialdehyde **10** with tripyrrane **13b**. The addition of longer chain substituents considerably improved the solubility of this system and allowed detailed NMR analysis. The proton NMR spectrum of **7b** (Figure 3) showed a broad peak between 3.45 and 3.07 ppm that correlated with an $sp^2$ carbon resonance at 128.7 ppm in the HSQC spectrum (Figure 4), and this was assigned to the internal CH. In addition, a second broad peak could be seen in some spectra near 4.6 ppm that corresponded to the NH.

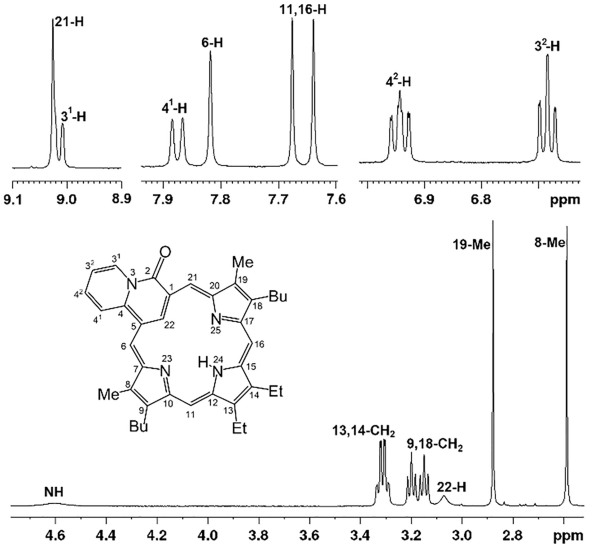


**Figure 3.** Partial $^1$H NMR spectrum of oxyquinoliziniporphyrin **7b**.

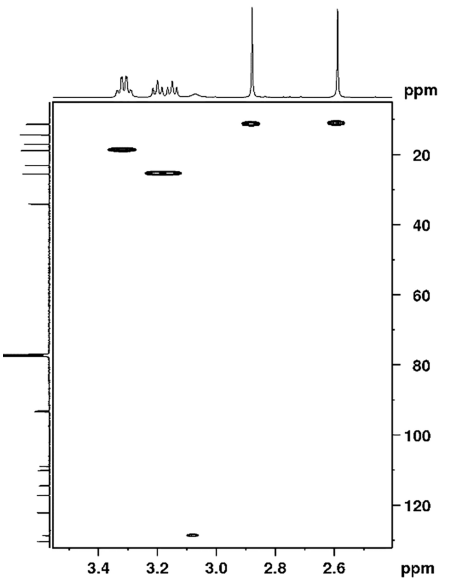


**Figure 4.** Partial HSQC NMR spectrum of **7b** in $CDCl_3$ showing a correlation between a broad peak in the proton NMR spectrum at 3.1 ppm with a carbon-13 resonance at 128.7 ppm.

These results indicate that oxyquinoliziniporphyrins have a global diatropic ring current, although this was much smaller than is seen for regular porphyrins or carbaporphyrins such as **2**. Furthermore, the UV−vis spectra of free base oxyquinoliziniporphyrins do not resemble the spectra for aromatic porphyrinoids. Instead of the strong Soret bands seen in fully aromatic systems, four medium-sized peaks were observed between 330 and 490 nm (Figure 5). Broad absorptions were

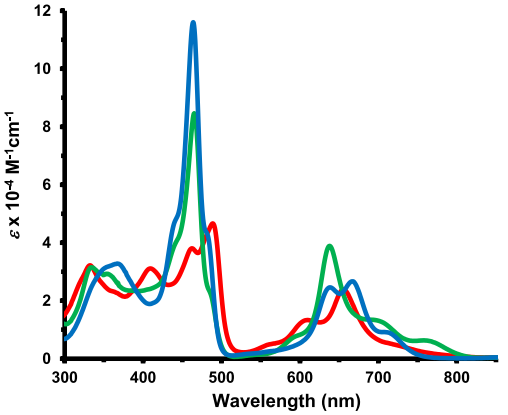


**Figure 5.** UV−vis spectra of oxyquinoliziniporphyrin **7b** in 1% $Et_3N$−$CH_2Cl_2$ (red line), in $CH_2Cl_2$ with 1 equiv TFA (green line), and in 10% TFA-$CH_2Cl_2$ (blue line).

also noted between 550 and 750 nm. The spectra are actually surprisingly similar to the electronic absorption spectra for azuliporphyrins **3**, an important class of carbaporphyrinoids with intermediary aromatic characteristics.[4] The internal protons for azuliporphyrins could not be identified in early investigations due to poor solubility,[4] but substituted systems (**3**, R = *t*-Bu or Ph) showed the inner CH resonance between 2.49 and 3.23 ppm, values that are again strikingly similar to those seen for **7b**. Global aromaticity in **7** is compromised by cross-conjugation and the presence of an amide subunit that can favor localized quinolizinium character (contributor **7′**). A



https://doi.org/10.1021/acs.orglett.2c02098
Org. Lett. 2022, 24, 5402−5406

degree of aromatic character may result from dipolar resonance contributors such as 7″ or the presence of species with [17]annulene anionic character (structure 7[h]). In both cases, these contrubutions would be limited due to the requirement for charge separation.

Addition of 1 equiv of TFA to solutions of **7a** or **7b** in $CH_2Cl_2$ afforded greatly altered UV−vis spectra with a Soret band at 465 nm and Q bands at 638, 700, and 763 nm (Figure 5), and this was attributed to the formation of monocations $7H^+$ (Scheme 3). The enhanced aromatic character of these

**Scheme 3. Protonation and Metalation of Oxyquinoliziniporphrins**

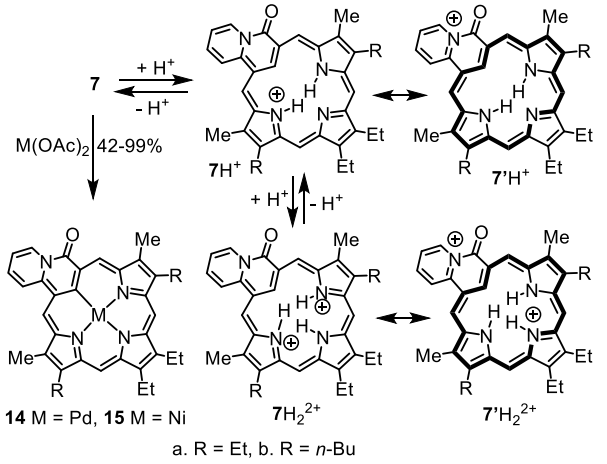


species is most likely due to resonance contributors such as $7'H^+$ that have porphyrin-like 18$\pi$ electron delocalization pathways while aiding in charge delocalization. Further addition of TFA led to an enhancement of the Soret band and the appearance of Q bands at 642, 671, and 717 nm (Figure 5). This was assigned to the formation of dications $\mathbf{7a,b}H_2^{2+}$ (Scheme 3). The proton NMR spectrum for $\mathbf{7a}H_2^{2+}$ in TFA−$CDCl_3$ also reflected greatly increased aromatic character as the external *meso*-protons appeared downfield at 10.35, 10.09, 9.28, and 9.25 ppm, while the internal CH was strongly shifted upfield to −3.07 ppm. Three NH resonances were identified at 1.14, 0.80, and −1.66 ppm. In the carbon-13 NMR spectrum, the internal CH gave a resonance at 119.2 ppm, while the *meso*-carbons appeared at 116.0, 112.3, 94.4, and 93.9 ppm. The increased diatropicity in $7H_2^{2+}$ might again be attributed to canonical forms such as $7'H_2^{2+}$ that possess porphyrin-like conjugation pathways.

Metalation of oxyquinoliziniporphyrins **7a** and **7b** was also investigated (Scheme 3). Reaction with palladium(II) acetate in $CHCl_3$−$CH_3CN$ occurred rapidly at room temperature (5−10 min) and afforded good yields of palladium(II) complexes **14**, although longer reaction times resulted in some decomposition. Nickel(II) acetate also reacted to give nickel(II) derivatives **15**, but it was necessary to carry out these reactions under refluxing conditions in $CHCl_3$−MeOH or $CHCl_3$−$CH_3CN$. The UV−vis spectra of palladium complexes **14** gave three absorption bands between 347 and 465 nm and a strong absorption in the Q-band region at 648 nm (Figure 6). The UV−vis spectra for the corresponding nickel complexes were similar, although the three absorptions in the Soret band region were broader and less resolved (Figure 6). These results indicate that these complexes do not

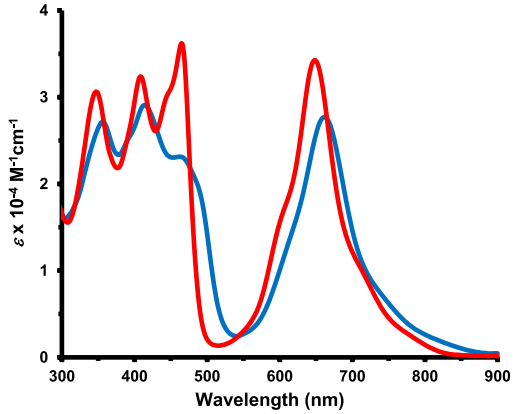


**Figure 6.** UV−vis spectra of palladium(II) complex **14a** (red line) and nickel(II) complex **15a** (blue line) in $CH_2Cl_2$.

possess strongly aromatic properties. The proton NMR spectrum of **14b** showed *meso*-protons at 9.48 (21-H), 8.36, 8.23, and 7.76 ppm. Even taking into account that the 21-H resonance is further deshielded by the proximity of the carbonyl unit, the results suggest that the palladium complexes have slightly increased diatropic ring currents compared to **7**. Nickel complex **15b** showed the equivalent resonances at 8.97, 8.14, 8.01, and 7.96 ppm, on balance indicating a slightly reduced aromatic ring current compared to its palladium counterpart.

In order to further assess the conformations and aromatic characteristics of oxyquinoliziniporphyrins, DFT studies were conducted on the unsubstituted system **16**. The relative energies of three tautomers, **16**, **16a**, and **16b** (Figure 7), were

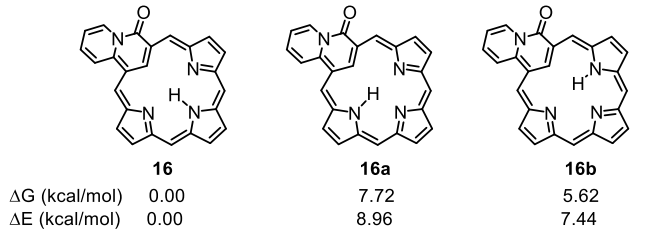


**Figure 7.** Relative energies of oxyquinoliziniporphyrin tautomers.

considered, and the most stable form was identified as **16**. Geometry optimization was performed using M06-2X with a 6-311++G** basis set, and complete results are disclosed in the Supporting Information. Tautomers **16** and **16b** are near planar, although minor distortions are evident in **16a** (Table S5). Oxyquinoliziporphyrin **16** shows extensive bond length alternation that is not consistent with an aromatic species (Figure 8). Six monoprotonated and four diprotonated species were also considered, and the lowest energy forms were shown to be $\mathbf{16}H^+$ and $\mathbf{16}H_2^{2+}$ (Table 1). Both of these structures exhibited substantial ring deformation (Table S5). The aromatic character of **16**, $\mathbf{16}H^+$, and $\mathbf{16}H_2^{2+}$ was assessed using nucleus-independent chemical shift (NICS) calculations.[12] NICS(0) and $NICS_{zz}(1)$ calculations were conducted (Tables 1 and S1−3). Standard NICS calculations consider the effects due to $\sigma$ and $\pi$ electrons, but $NICS_{zz}$, performed 1 Å above the ring, primarily measures the effects due to the $\pi$ system, and this method is considered to be a more accurate probe for aromatic character. Measurements were made in the middle of the macrocycle and separately for each individual


https://doi.org/10.1021/acs.orglett.2c02098
Org. Lett. 2022, 24, 5402−5406

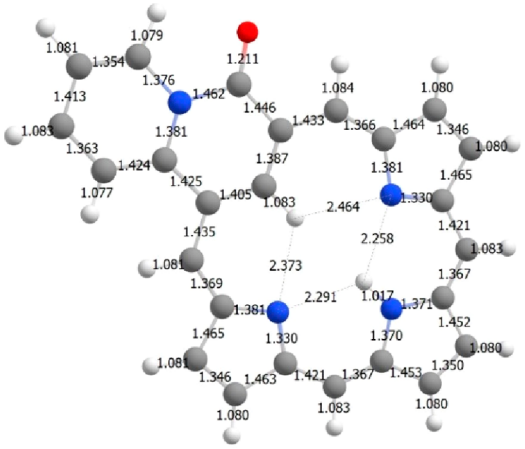


**Figure 8.** Calculated bond lengths (Å) for **16**.

**Table 1. NICS and NICS$_{zz}$ values for Unsubstituted Oxyquinoliziniporphyrin 7 and Related Mono- and Dicationic Species**[a]

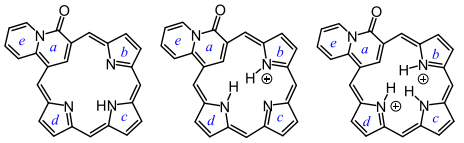

| | **16** | **16**H$^+$ | **16**H$_2^{2+}$ |
|---|---|---|---|
| NICS(0)/NICS(01)$_{zz}$ | -4.61/-10.62 | -9.91/-24.47 | -11.43/-26.85 |
| NICS(a)/NICS(a1)$_{zz}$ | +0.35/-2.52 | +3.05/+3.63 | +5.95/+9.43 |
| NICS(b)/NICS(b1)$_{zz}$ | -1.64/-10.63 | -9.77/-24.48 | -12.39/-24.11 |
| NICS(c)/NICS(c1)$_{zz}$ | -5.45/-14.67 | +0.32/-8.99 | -10.60/-39.27 |
| NICS(d)/NICS(d1)$_{zz}$ | -1.94/-11.15 | -9.57/-20.74 | -12.18/-20.54 |
| NICS(e)/NICS(e1)$_{zz}$ | -3.31/-13.37 | -4.80/-18.14 | -5.38/-19.93 |

[a]In each case, the structures correspond to the most stable tautomers.

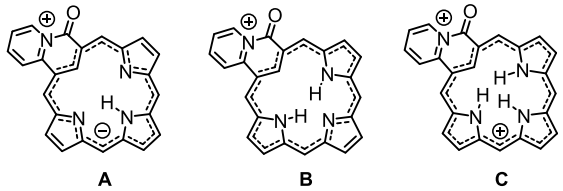


**Figure 9.** Potential $\pi$ electron circuits in **16** and related protonated species. (A) Possible 17-atom circuit in **16**. (B) Favored 18$\pi$ electron pathway for **16**H$^+$. (C) Important 19-atom 18$\pi$ electron circuit in dication **16**H$_2^{2+}$.

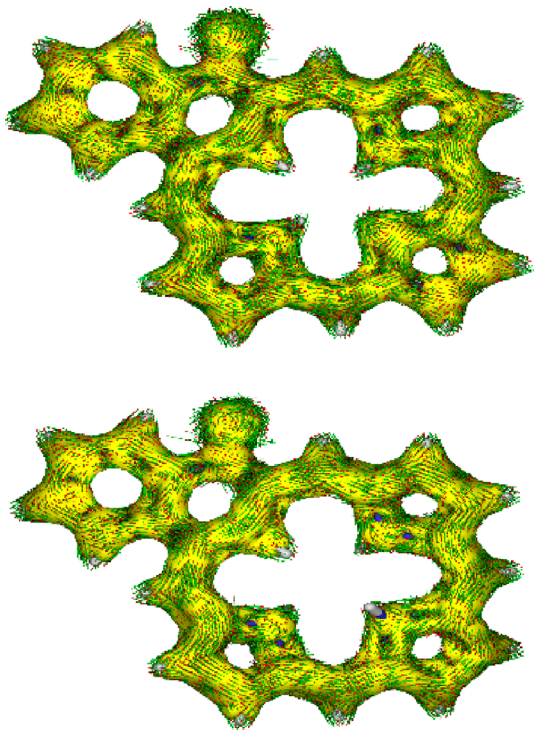

**Figure 10.** AICD plots (isovalue = 0.05) of unsubstituted oxyquinoliziniporphyrin monocation **16**H$^+$ (above) and dication **16**H$_2^{2+}$ (below).

ring. Negative values are indicative of significant shielding effects, although the numerical values obtained using NICS$_{zz}$(1) are much larger than the results for NICS(0). The values for **16** shows the presence of a moderate global ring current, and rings *b*, *c*, and *d* also show weak or moderate shielding effects. These data do not demonstrate the presence of specific aromatic circuits, and anisotropy of induced current density (AICD) plots[13] (Figure S70) also showed bifurcated pathways. Although the 18$\pi$ electron pathway shown in **7″** is one explanation, other possibilities include the 17-atom 18$\pi$ electron circuit shown in structure **A** (Figure 9). Monocation **16**H$^+$ shows a greatly increased diatropic ring current, and rings *b*, *d* and *e* are also strongly shielded. This is consistent with a major delocalization pathway running around the outside of rings *b* and *d* and the inside of rings *a* and *c* as illustrated in structure **B** (Figure 9); ring *e* takes on pyridinium-like properties. This interpretation is confirmed by the AICD plot for **16**H$^+$ (Figure 10). Dication **16**H$_2^{2+}$ shows a slightly increased ring current, but rings *b*, *c*, *d* and *e* are all strongly shielded, showing that a 19-atom circuit (structure **C** in Figure 9) is favored for this species, and this interpretation is again supported by the AICD plot (Figure 10).

This study demonstrates that insertion of a quinolizone subunit into a porphyrinoid structure leads to profound spectroscopic changes, although some global aromatic character is retained. Protonation drastically increases the aromaticity of this system and results in the production of strong diatropic ring currents as assessed by proton NMR spectroscopy, NICS calculations, and AICD plots. Organometallic derivatives were easily synthesized with Ni(II) or Pd(II), and these stable complexes gave strong absorptions at longer wavelengths (>600 nm). The embedded external nitrogen substantially modifies the properties of this system, and these results point the way toward further modified systems with external heteroatoms.

## ■ ASSOCIATED CONTENT

### Supporting Information

The Supporting Information is available free of charge at https://pubs.acs.org/doi/10.1021/acs.orglett.2c02098.



https://doi.org/10.1021/acs.orglett.2c02098
Org. Lett. 2022, 24, 5402−5406

Experimental procedures, characterization, and copies of selected UV−vis, $^{1}$H NMR, $^{1}$H−$^{1}$H COSY, HSQC, DEPT-135, $^{13}$C{$^{1}$H} NMR, and mass spectra (PDF)

## AUTHOR INFORMATION


### Corresponding Author

**Timothy D. Lash** − *Department of Chemistry, Illinois State University, Normal, Illinois 61790-4160, United States;* orcid.org/0000-0002-0050-0385; Email: tdlash@ilstu.edu

### Authors

**Emma K. Cramer** − *Department of Chemistry, Illinois State University, Normal, Illinois 61790-4160, United States*

**Deyaa I. AbuSalim** − *Department of Chemistry, Illinois State University, Normal, Illinois 61790-4160, United States*

Complete contact information is available at: https://pubs.acs.org/10.1021/acs.orglett.2c02098


### Notes

The authors declare no competing financial interest.

## ACKNOWLEDGMENTS

This work was supported by the National Science Foundation under grant CHE-1855240. The NSF is also acknowledged for providing funding for the departmental NMR spectrometers (CHE-0722385) and mass spectrometer (CHE-1337497) under the Major Research Instrumentation (MRI) program.

## REFERENCES


(1) Lash, T. D. Carbaporphyrinoid Systems. *Chem. Rev.* **2017**, *117*, 2313−2446.

(2) Lash, T. D.; Colby, D. A.; Szczepura, L. F. New Riches in Carbaporphyrin Chemistry: Silver and Gold Organometallic Complexes of Benzocarbaporphyrins. *Inorg. Chem.* **2004**, *43*, 5258−5267.

(3) Adiraju, V. A. K.; Ferrence, G. M.; Lash, T. D. Rhodium(I), Rhodium(III) and Iridium(III) Carbaporphyrins. *Dalton Trans.* **2016**, *45*, 13691−13694.

(4) (a) Lash, T. D.; Chaney, S. T. Azuliporphyrin: A Case of Borderline Porphyrinoid Aromaticity. *Angew. Chem., Int. Ed. Engl.* **1997**, *36*, 839−840. (b) Lash, T. D.; El-Beck, J. A.; Ferrence, G. M. Synthesis and Reactivity of *meso*-Unsubstituted Azuliporphyrins Derived from 6-*tert*-Butyl- and 6-Phenylazulene. *J. Org. Chem.* **2007**, *72*, 8402−8415. (c) Lash, T. D. Out of the Blue! Azuliporphyrins and Related Carbaporphyrinoid Systems. *Acc. Chem. Res.* **2016**, *49*, 471−482.

(5) (a) Stepien, M.; Latos-Gražyński, L. Benziporphyrins: Exploring Arene Chemistry in a Macrocyclic Environment. *Acc. Chem. Res.* **2005**, *38*, 88−98. (b) Lash, T. D. Benziporphyrins, a Unique Platform for Exploring the Aromatic Characteristics of Porphyrinoid Systems. *Org. Biomol. Chem.* **2015**, *13*, 7846−7878.

(6) (a) Srinivasan, A.; Furuta, H. Confusion Approach to Porphyrinoid Chemistry. *Acc. Chem. Res.* **2005**, *38*, 10−20. (b) Toganoh, M.; Furuta, H. Creation from Confusion to Fusion in the Porphyrin World - The Last Three Decades of N-Confused Porphyrinoid Chemistry. *Chem. Rev.* **2022**, *122*, 8313−8437.

(7) (a) Latos-Grażyński, L. In *The Porphyrin Handbook*; Kadish, K. M., Smith, K. M., Guilard, R., Eds.; Academic Press: San Diego, 2000; Vol. *2*, pp 361−416. (b) Chmielewski, P. J.; Latos-Grażyński, L. Core Modified Porphyrins − A Macrocyclic Platform for Organometallic Chemistry. *Coord. Chem. Rev.* **2005**, *249*, 2510−2533. (c) Thuita, D. W.; Brückner, C. Metals Complexes of Porphyrinoids Containing Nonpyrrolic Heterocycles. *Chem. Rev.* **2022**, *122*, 7990−8052. (d) Lash, T. D. *Heteroporphyrins and Carbaporphyrins in Fundamentals of Porphyrin Chemistry - A 21st Century Approach*; Brothers, P., Senge, M., Eds.; Wiley: Hoboken, 2022; Vol. *1*, Chapter 8, pp 385−451.

(8) Young, A. M.; Von Ruden, A. L.; Lash, T. D. Pyrazole Analogues of Porphyrins and Oxophlorins. *Org. Biomol. Chem.* **2011**, *9*, 6293−6305.

(9) (a) Myśliborski, R.; Latos-Grażyński, L. Carbaporphyrinoids Containing a Pyridine Moiety: 3-Aza-*meta*-benziporphyrin and 24-Thia-3-aza-*meta*-benziporphyrin. *Eur. J. Org. Chem.* **2005**, *2005*, 5039−5048. (b) Lash, T. D.; Pokharel, K.; Serling, J. M.; Yant, V. R.; Ferrence, G. M. Aromatic and Nonaromatic Pyriporphyrins. *Org. Lett.* **2007**, *9*, 2863−2866.

(10) Jones, G. Aromatic Quinolizines. *Adv. Heterocycl. Chem.* **1982**, *31*, 1−62.

(11) Boekelheide, V.; Lodge, J. P., Jr. A Study of Some Quinolizone Derivatives. *J. Am. Chem. Soc.* **1951**, *73*, 3681−3684.

(12) Chen, Z.; Wannere, C. S.; Corminboeuf, C.; Puchta, R.; Schleyer, P. v. R. Nucleus-independent Chemical Shifts (NICS) as an Aromaticity Criterion. *Chem. Rev.* **2005**, *105*, 3842−3888.

(13) Geuenich, D.; Hess, K.; Köhler, F.; Herges, R. Anisotropy of the Induced Current Density (ACID), a General Method to Quantify and Visualize Electronic Delocalization. *Chem. Rev.* **2005**, *105*, 3758−3772.






https://doi.org/10.1021/acs.orglett.2c02098
*Org. Lett.* 2022, 24, 5402−5406